

Analytical Study of Light Scattering Characteristics of Radially Inhomogeneous Subwavelength Spheres

Dimitrios C. Tzarouchis and Ari Sihvola
 Department of Electronics and Nanoengineering, Aalto University,
 Maarintie 8, 02150, Espoo, Finland

Abstract

In this work the electrostatic problem of a subwavelength core-shell sphere exhibiting a radially inhomogeneous permittivity profile is considered. The general mathematical treatment for the electrostatic polarizability will be presented in terms of scattering potentials. The case of a power-law profile and a new class of permittivity profiles that exhibit an exponential-radial dependence are considered. The presented theoretical results can open multiple avenues towards the exploration/implementation of scatterers with more exotic permittivity profiles for RF/optics and remote sensing applications.

1 Introduction

Electromagnetic scattering by subwavelength spheres is a canonical and fundamental problem found in the core of many areas such as RF/optical engineering, bioengineering, and material sciences [1, 2, 3]. In this work the concept of the polarizability is refined by assuming a more general case of a sphere with a radially inhomogeneous (graded-index, or RI) permittivity profile. This kind of profiles occur either naturally or artificially [4, 5].

Here, the electrostatic problem of a radially inhomogeneous sphere (RI) will be considered. A new family of permittivity profiles with exact solution, i.e., exponential linear and inverse linear permittivity, will be introduced and presented. Results on the plasmonic resonances of these cases are given, exposing their main scattering trends. The analysis concludes with the validation of the presented results by comparing the scattering response with a multilayer sphere approximating the corresponding RI profiles. It is estimated that the presented results will stimulate further discussions for the theory of RI scatterers and their functionalities, enabling their experimental implementation for modern energy control/harvesting applications.

2 Short theory

Let us assume a sphere (Fig. 1, with subscript 0 for external, 1 for shell, and 2 for core domain) of radii r_1 and r_2 , subject

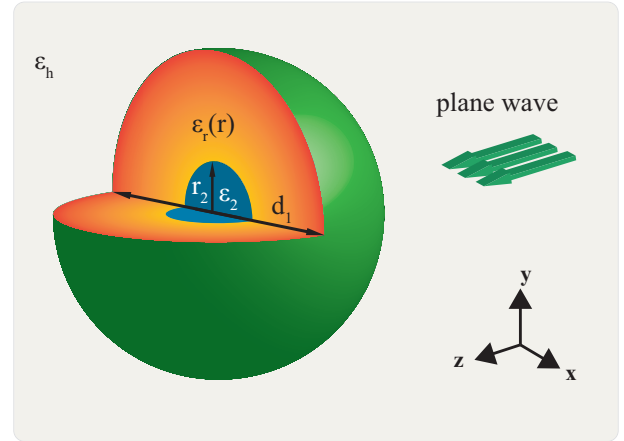


Figure 1. A radially inhomogeneous sphere of diameter $d_1 = 2r_1$, with an internal homogeneous core of radius r_2 and ϵ_2 immersed in a host medium (ϵ_h) subject to a plane wave (constant excitation field in the long wave approximation).

to a uniform electrostatic field causing a scattering field of dipolar character, and the internal fields described as

$$\begin{aligned} \mathbf{E}_0(r, \theta) &= E_0 \mathbf{u}_z + \frac{B_0}{r^3} (2 \cos \theta \mathbf{u}_r + \sin \theta \mathbf{u}_\theta) \\ \mathbf{E}_1(r, \theta) &= -f'(r) \cos \theta \mathbf{u}_r + f(r) \frac{\sin \theta}{r} \mathbf{u}_\theta \\ \mathbf{E}_2(r, \theta) &= -A_2 \mathbf{u}_z \end{aligned} \quad (1)$$

where $\mathbf{u}_z = \cos \theta \mathbf{u}_r - \sin \theta \mathbf{u}_\theta$. We assume that the arbitrary radial function $f(r)$ provides a valid solution for the formulated problem in region 1; a key step towards the generalization of the problem. Both expressions of the scattered and the internal (core) field are divergenceless, satisfying all the requirements of the corresponding physical problem, i.e., the scattered field vanishes at large distances with no singularities at the origin [6]. Similarly the field in region one should be divergenceless, viz.,

$$\nabla \cdot \mathbf{D}_1 = \nabla \cdot (\epsilon_r(r) \mathbf{E}_1(r, \theta)) = 0 \quad (2)$$

resulting to the following O.D.E

$$f''(r) + \left(\frac{2}{r} + \frac{\epsilon_r'(r)}{\epsilon_r(r)} \right) f'(r) - \frac{2}{r^2} f(r) = 0 \quad (3)$$

Here we present the cases where Eq. (3) obtains a closed form solution. For these cases one can express the radial function as

$$f(r) = A_1 A(r) + B_1 B(r) \quad (4)$$

where $A(r)$ is a constant-like and $B(r)$ is a dipole-type solutions of the radial function. For instance for the case of a homogeneous profile we have $A(r) = r$ and $B(r) = \frac{1}{r^2}$, implying that $A(r)$ is well-behaving at the origin and $B(r)$ contains a singularity. However this is not always true, since $A(r)$ and $B(r)$ can both exhibit a singular behavior, for example for the exponential permittivity profile. In that case special mathematical treatment is required, e.g., introduction of a singularity subtracting region at the center.

The unknown scattering amplitudes, B_0, A_1, B_1 , and A_2 , can be evaluated by applying the continuity of the tangential electric field and normal flux density components. The formulated linear system can be compactly expressed in a matrix form $\mathbf{A}\bar{\mathbf{X}} = \mathbf{b}$ for which the four unknowns are $\bar{\mathbf{X}} = (B_0 \ A_1 \ B_1 \ A_2)^T$, and the system matrix and excitation vector read

$$\mathbf{A} = \begin{pmatrix} -\frac{1}{r_1^2} & A(r_1) & B(r_1) & 0 \\ \frac{2\varepsilon_0}{r_1^3} & \varepsilon_r(r_1)A'(r_1) & \varepsilon_r(r_1)B'(r_1) & 0 \\ 0 & A(r_2) & B(r_2) & -r_2 \\ 0 & \varepsilon_r(r_2)A'(r_2) & \varepsilon_r(r_2)B'(r_2) & -\varepsilon_2 \end{pmatrix} \quad (5)$$

$$\mathbf{b} = -E_0 \begin{pmatrix} r_1 \\ \varepsilon_0 \\ 0 \\ 0 \end{pmatrix} \quad (6)$$

Note that primes denote the differentiation with respect to r . The determination of the scattering amplitudes in each region is reduced to a brute force matrix inversion.

2.1 Linear Exponential profile e^{nr}

The first profile under examination is the linear exponential profile, i.e.,

$$\varepsilon_r(r) = \varepsilon_1 e^{nr} \quad (7)$$

where n can be any arbitrary real parameter with units [1/m]. The formulated O.D.E is

$$f''(r) + \frac{1}{r}(nr+2)f'(r) - \frac{2}{r^2}f(r) = 0 \quad (8)$$

and its solution, expressed in terms of the corresponding $A(r)$ and $B(r)$ functions, reads

$$A(r) = \frac{1}{n} \left(1 - \frac{2}{nr} + \frac{2}{n^2 r^2} \right) \quad (9)$$

and

$$B(r) = \frac{e^{-nr}}{r^2} \quad (10)$$

where both $A(r)$ and $B(r)$ are singular at the origin.

2.2 Inverse-linear exponential profile $e^{\frac{1}{nr}}$

In this case the inhomogeneity can be expressed as

$$\varepsilon_r(r) = \varepsilon_1 e^{\frac{1}{nr}} \quad (11)$$

with a n being an arbitrary constant, similar to the exponential profile. The formulated O.D.E reads

$$f''(r) + \frac{1}{nr^2}(2nr-1)f'(r) - \frac{2}{r^2}f(r) = 0 \quad (12)$$

and the associated functions are

$$A(r) = \frac{2nr}{2n-1} \quad (13)$$

and

$$B(r) = \frac{n+2n^2r}{1-2n} e^{-\frac{1}{nr}} \quad (14)$$

In most of the cases $A(r)$ is a well-behaving function at the origin ($r=0$), while $B(r)$ contains a singularity. This observation, however, does not hold for every solvable case, for example the exp profile where both equations $A(r)$ and $B(r)$ are singular at the origin. A singularity extracting region at the origin (core) is therefore required for the calculating the polarizability of the core-shell inclusion; the intact case can be reached by taking the limiting case where the core size radius is zero.

3 Discussion and Conclusions

A first step to test the correctness of the results can be performed by considering the simplest case of an intact inhomogeneous particle. In this case the polarizability is

$$B_0^{cs} = \frac{C\varepsilon_1 - \varepsilon_0}{C\varepsilon_1 + 2\varepsilon_0} E_0 r_1^3 \quad (15)$$

with

$$C = r_1 \frac{A'(r_1)}{A(r_1)} \quad (16)$$

being the inhomogeneity factor.

3.1 Core-shell homogeneous profile

For example a homogeneous case has an inhomogeneity factor $C = 1$, since $A(r) = r$. A more general case is a homogeneous core-shell particle that can be seen as a sphere with step-wise inhomogeneous profile, with $A(r) = r$ and $B(r) = \frac{1}{r^2}$. In this case the polarizability reads [7, 8]

$$B_0^{cs} = \frac{C\varepsilon_1 - \varepsilon_0}{C\varepsilon_1 + 2\varepsilon_0} E_0 r_1^3 \quad (17)$$

where the introduced inhomogeneity factor is

$$C = -2 + 3 \frac{1}{1 - \frac{\varepsilon_2 - \varepsilon_1}{\varepsilon_2 + 2\varepsilon_1} \eta^3} \quad (18)$$

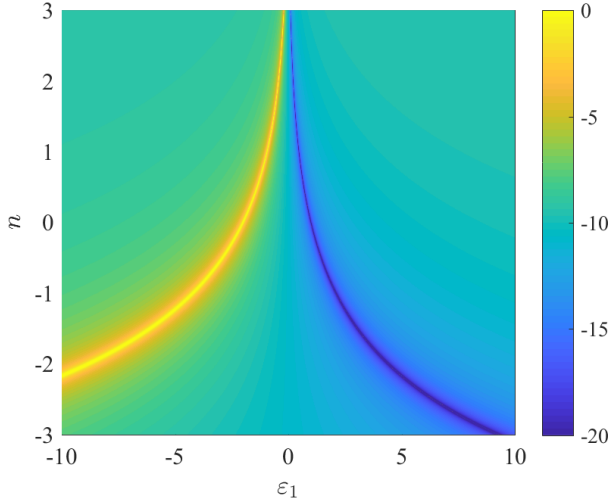


Figure 2. Scattering efficiency (in logarithmic scale) of the linear exponential permittivity profiles as a function of the scaling factor n and the internal permittivity ε_1 .

and $\eta = \frac{r_2}{r_1}$ is the radius ratio. The scaling factor C approaches unity when either $\eta = 0$ (no core) or the contrast between the core and shell permittivity is zero ($\varepsilon_1 - \varepsilon_2 = 0$). On the other hand $C = \frac{\varepsilon_2}{\varepsilon_1}$ for $\eta \rightarrow 1$. One can observe that with some mathematical manipulations the above expression leads to the well-known polarizability for a core-shell sphere

$$B_0^{cs} = \frac{(\varepsilon_0 - \varepsilon_1)(2\varepsilon_1 + \varepsilon_2) + \eta^3(\varepsilon_0 + 2\varepsilon_1)(\varepsilon_1 - \varepsilon_2)}{(2\varepsilon_0 + \varepsilon_1)(2\varepsilon_1 + \varepsilon_2) + 2\eta^3(\varepsilon_0 - \varepsilon_1)(\varepsilon_1 - \varepsilon_2)} E_0 r_1^3 \quad (19)$$

3.2 Exponential profiles

To illustrate the scattering peculiarities of an RI sphere with exponential profile we analyze the case of an intact sphere. As can be seen already from their mathematical treatment, these particular profiles require the existence of a regularization core region, and hence the results of an intact sphere can be only approached by applying the $\eta \rightarrow 0$ limit to the polarizability. Starting with the linear exp profile, e^{nr} , the inhomogeneity factor leads to

$$C_e = 2 \frac{e^{nr_1} (nr_1 - 2) + nr_1 + 2}{e^{nr_1} (n^2 r_1^2 - 2nr_1 + 2) - 2} \quad (20)$$

where for $n \rightarrow 0$ we have $C_{\text{exp}} = 1$. In a similar manner, the inverse linear exponential profile gives an inhomogeneity factor of the form

$$C_{ie} = \begin{cases} 1 + \frac{1}{nr_1} - \frac{1}{1+2nr_1} & , n > 0 \\ \frac{2nr_1}{1-2nr_1} & , n \leq 0 \end{cases} \quad (21)$$

Note that this form depends of the sign of the parameter n . One observes that for the exp case (Fig 2), large positive values of n shift both the zero and the pole of the polarizability to the ENZ limit, while for $n < 0$ the plasmonic

resonance is rapidly shifted towards negative smaller values of ε_1 . The inv-exp case (Fig 3) reveals that the trend observed in the exp case is inverted. For instance, small values of positive n result in the collapse of both pole and zero at the ENZ limit. On the other hand small (negative) values of n shift extremely the resonance.

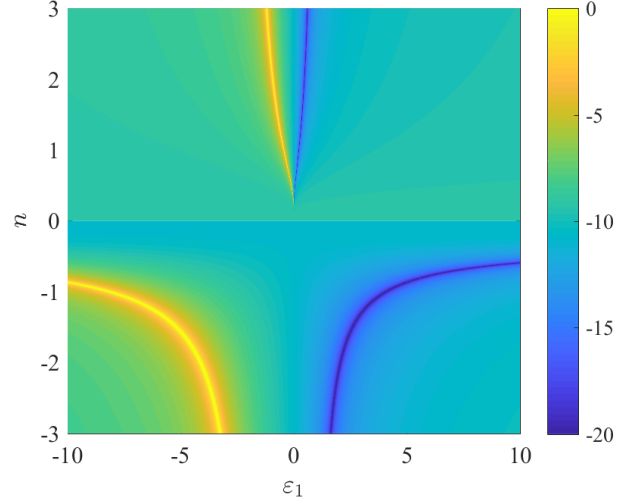


Figure 3. Scattering efficiency (in logarithmic scale) of the inverse-linear exponential permittivity profiles as a function of the scaling factor n and the internal permittivity ε_1 .

4 Conclusions

In this presentation the concept of the polarizability has been generalized, allowing us to rigorously explore the non-trivial physical mechanisms for a whole new family of graded-index particles. The simplified polarizability description can be used for reverse-engineering the inhomogeneity coefficient C for fitting the experimental data, paving the way for an alternative explanation of experimentally observed deviations of the plasmonic resonances on deeply subwavelength spheres [9].

The introduced description can be also implemented for a wide range of practical cases such as the accurate modeling of inhomogeneous structures (stratified spheres, transformation optics [10]), the implementation of temperature gradients (via a varying permittivity profile), the modeling of diffusive effects especially between interfaces or for extremely small particles [9], where interfaces are not hard but rather follow a radially dependent distribution. It is envisioned that the presented study will stimulate novel energy control/harvesting ideas for nanophotonic applications, such as the implementation of subwavelength plasmonic particles exhibiting Luneburg, Eaton, or more exotic graded-index profiles.

5 Acknowledgements

The authors would like to acknowledge support from the Nokia Foundation and the Aalto ELEC Doctoral School.

References

- [1] R. A. Shore, "Scattering of an electromagnetic linearly polarized plane wave by a multilayered sphere: Obtaining a computational form of Mie coefficients for the scattered field." *IEEE Antennas Propag. Mag.*, vol. 57, no. 6, pp. 69–116, Dec 2015.
- [2] M. E. Stewart, C. R. Anderton, L. B. Thompson, J. Maria, S. K. Gray, J. A. Rogers, and R. G. Nuzzo, "Nanostructured plasmonic sensors," *Chem. Rev.*, vol. 108, no. 2, pp. 494–521, 2008.
- [3] A. Krasnok, M. Caldarola, N. Bonod, and A. Alú, "Spectroscopy and biosensing with optically resonant dielectric nanostructures," *Adv. Opt. Mater.*, p. 1701094, Jan 2018.
- [4] J. Cai, J. P. Townsend, T. C. Dodson, P. A. Heiney, and A. M. Sweeney, "Eye patches: Protein assembly of index-gradient squid lenses," *Science (80-.)*, vol. 357, no. 6351, pp. 564 LP – 569, 2017.
- [5] T. Zentgraf, Y. Liu, M. H. Mikkelsen, J. Valentine, and X. Zhang, "Plasmonic Luneburg and Eaton lenses," *Nat Nano*, vol. 6, no. 3, pp. 151–155, 2011.
- [6] J. D. Jackson, *Classical Electrodynamics*. Wiley Online Library, 1975.
- [7] A. Sihvola and I. V. Lindell, "Transmission line analogy for calculating the effective permittivity of mixtures with spherical multilayer scatterers," *J. Electromagn. Waves Appl.*, vol. 2, no. 8, pp. 741–756, 1988.
- [8] D. Tzarouchis and A. Sihvola, "Light scattering by a dielectric sphere: Perspectives on the Mie resonances," *Appl. Sci.*, vol. 8, no. 2, 2018.
- [9] T. Christensen, W. Yan, S. Raza, A.-P. Jauho, N. A. Mortensen, and M. Wubs, "Nonlocal response of metallic nanospheres probed by light, electrons, and atoms," *ACS Nano*, vol. 8, no. 2, pp. 1745–1758, 2014.
- [10] A. Vakil and N. Engheta, "Transformation optics using graphene," *Science (80-.)*, vol. 332, no. 6035, pp. 1291 LP – 1294, 2011.